

On-line implementation of decoupled input-output linearizing controller in Baker's yeast fermentation

Viki R. Chopda¹, Anurag S. Rathore¹, James Gomes²

¹Chemical Engineering Department, Indian Institute of Technology, Hauz Khas, New Delhi 110016, India
(vikichopda@gmail.com, asrathore@biotechmz.com)

²School of Biological Sciences, Indian Institute of Technology Delhi, Hauz Khas, New Delhi 110016, India
(jgomes@bioschool.iitd.ac.in)

Abstract: Baker's yeast fermentation is influenced by the relative concentration of glucose and dissolved oxygen (DO) in the reactor. The process is sensitive to the oxidative capacity of the cells and exhibits a range of metabolic regimes depending on available glucose and oxygen. The time profiles of cell mass, glucose, ethanol and DO concentrations possess strong nonlinear characteristics. A decoupled input-output linearizing controller (DIOLC), which exhibited satisfactory performance in simulation experiments, was implemented online for validation. Our results showed that the DIOLC was capable of negating the interaction between glucose and dissolved oxygen, and executed satisfactory control action in experiments carried out in a 5 liter bioreactor. The performance of DIOLC was better compared to that of a PID controller implemented under identical test conditions.

Keywords: yeast fermentation, nonlinear control, decoupling, input-output linearization, PID control

1. Introduction

Conversion of glucose to ethanol or biomass by yeasts has been the core of the wine and bakery industry for centuries. Recently, the process of ethanol synthesis by yeasts has been revisited to exploit the potential of yeasts and develop methods for improving ethanol production from renewal resources to replenish to some degree the worsening fuel shortage. Researchers across the world are actively investigating the genetic circuitry of the yeast, to develop strains that produce a variety of biological products to meet pre-defined objectives. Baker's yeast has been used extensively for the enzymes, antibiotics, growth hormones, single cell proteins and amino acids. For these reasons, and the fact that yeasts exhibit a wide range of metabolic behaviour, fed-batch yeast production is a preferred process for testing new process methodologies and control strategies.

Various control strategies including those based on neural networks, adaptive models and fuzzy logic have been routinely validated on the fed-batch yeast fermentation process. Ławryńczuk (2011) developed a model predictive controller combined with an adaptive steady-state target optimization. A fuzzy control system was developed by Karakuzu et al. (2005), in which they employed two ANN estimators for on-line computing of biomass concentration and specific growth rate. The molasses and air feed rate were the inputs manipulated to control the specific growth rate and the dissolved oxygen concentration along a desired trajectory. In another study, Renard and Wouwer (2008) developed 2 robust controllers based on the internal model principle. They used the Sonnleitner-Kapelli (1986) model for developing these controllers. There are also examples of implementation

of feeding strategies such as logistic feeding (Miśkiewicz, T. and Borowiak, D., 2005) and pulsed feeding (Kasperski, A. and Miśkiewicz, T., 2008) to improve biomass productivity.

In this paper, we present the results of on-line implementation of the DIOLC for fed-batch yeast fermentation. In this strategy, we have used real-time measurements of DO and residual glucose concentration to control the process on-line while the cell mass and ethanol concentrations were measured offline. The interaction between the glucose and DO concentration was decoupled using a simple matrix inversion principle. The test experiments were simulated and these results were compared to the results obtained from online implementation. The performance of DIOLC was compared to that of a proportional-integral-derivative (PID) controller.

1.1 Model for Baker's yeast growth

The baker's yeast fermentation process was chosen for DIOLC implementation because it offers sufficient metabolic complexity for testing new controllers [Ostergaard, et al. 2000]. The growth of yeast on glucose depends on the oxidative capacity of the cells. Glucose is utilized by the oxidative route for growth as long as it does not saturate the oxidative capacity. If the glucose supplied is below the saturation concentration and if ethanol is present, the ethanol is used by the oxidative route. In this study, the model formulated by Sonnleitner and Kappeli (1986) for yeast fermentation has been used. The model is mechanistic and uses DO as a variable to describe the growth of yeast on both glucose and ethanol. The Sonnleitner and Kappeli model was rewritten in the state-space form with specific uptake rates

and modified to include the dilution terms for the fed-batch cultivation.

$$\begin{bmatrix} \dot{x} \\ \dot{s} \\ \dot{e} \\ \dot{c}_L \end{bmatrix} = \begin{bmatrix} (\alpha_1 - \alpha_3)\mu_1(s, c_L) + \alpha_2\mu_2(s) + \alpha_4\mu_3(s, e, c_L) \\ -\alpha_4\mu_2(s) \\ -\alpha_6\mu_1(s, c_L) + \alpha_2\mu_2(s) - \alpha_7\mu_3(s, e, c_L) \\ -\mu_1(s, c_L) - \mu_3(s, e, c_L) \end{bmatrix} x + \begin{bmatrix} -x & 0 \\ s_F - s & 0 \\ -e & 0 \\ -c_L & c_L^* - c_L \end{bmatrix} \begin{bmatrix} D \\ k_L a \end{bmatrix} \quad (1)$$

Where $x(t)$, $s(t)$, $e(t)$ and $c_L(t)$ are the biomass, glucose, ethanol and dissolved oxygen concentrations respectively that constitute the state variables of the process (X). The kinetics of the process (μ_i), possess the Monod structure and are described by the terms $\mu_1(s, c_L)$, $\mu_2(s)$ and $\mu_3(s, e, c_L)$ representing the oxidative growth on glucose, maximum growth on glucose and oxidative growth on ethanol respectively. The values of the model parameters are given in Table 3 (Appendix). These parameters were taken from literature (Sonnleitner and Kappeli, 1986) in which a range for each parameter was given. Using this model, we carried out a DoE exercise in which we performed simulations to determine the optimum values of these parameters. These parameters are validated through batch experiments and subsequently used in the controller design.

2. DIOLC derivation and stability analysis

The method of derivation of DIOLC is based on successive Lie differentiation and use of simple matrix inversion principle. Since two of the four state variables, s and c_L , were measured, and relative degree was first determined. The relative degrees r_1 and r_2 with respect to the outputs s and c_L is each equal to unity, resulting in a relative degree $r = 2$ for the system. Hence, the dynamics of the unmeasured variables x and e are not observable. Therefore, it is necessary to ensure that the system remains stable when s and c_L vary with time under the action of the control inputs. This insight is obtained by studying the zero dynamics, the dynamics of the unmeasured states x and e , when the measured outputs s and c_L are constrained to be exactly zero by the process inputs. In order to keep the outputs exactly zero, the control input must be chosen as

$$u^*(X) = -E^{-1}(X) \begin{bmatrix} L_j^r h_1(X) \\ \vdots \\ L_j^r h_m(X) \end{bmatrix} \quad (2)$$

Thus, for our system described by Eq. 1

$$u^*(X) = \begin{bmatrix} D^* \\ k_L a^* \end{bmatrix} = \begin{bmatrix} \frac{1}{s_F - s} & 0 \\ \frac{c_L}{(s_F - s)(c_L^* - c_L)} & \frac{1}{c_L^* - c_L} \end{bmatrix} \begin{bmatrix} -\alpha_4\mu_2(s)x \\ (-\mu_1(s, c_L)x) \\ (-\mu_3(s, e, c_L)x) \end{bmatrix} \quad (3)$$

Applying the constraints $s=c_L=0$, we obtain $D^*=0$. Substituting this back into Eq. 1, we get the zero dynamics for x and e as

$$\dot{x}^* = 0, \quad \dot{e}^* = 0 \quad (4)$$

When $s=c_L=0$ is applied on the system, the rate of change in biomass and ethanol becomes zero (Eq. 4) and hence the

concentrations of biomass and ethanol are bounded. When $c_L=0$ the oxidative growth on both glucose and ethanol is prohibited. The additional constraint of $s=0$ further restricts the reductive growth of yeast on glucose. Consequently, growth stops leading to a constant biomass concentration (x^*). In addition, since no ethanol is produced or utilized, the ethanol concentration becomes constant at e^* . The process effectively becomes stationary because the biomass and ethanol concentrations remain at the values they had at the instant when the zero dynamic condition was imposed. Therefore, the fed-batch growth of *Saccharomyces cerevisiae* is stable under the action of decoupled input-output linearizing controller. This has been proven by extensive simulations of the fed-batch growth of *S. cerevisiae*. The DIOLC gave stable performance under test conditions spanning a range of metabolic regimes [Persad, A. et al. 2013]. Figure 1 shows the basic principle of implementation for DIOLC.

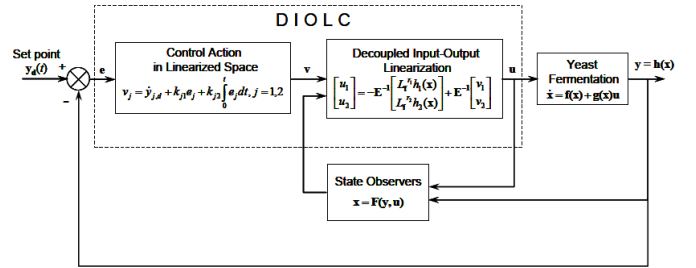


Fig. 1. Block diagram showing the implementation of DIOLC in a closed-loop configuration in yeast fermentation.

3. Tuning of controllers

The response of DIOLC and PID controllers to step changes in the s and c_L setpoints was simulated in different metabolic regimes. The sampling intervals for DO and substrate were taken as 30 sec and 2 min respectively, based on the duration required by the oxygen electrode and glucose analyzer to complete a measurement cycle. The simulations were carried out to determine a range of tuning parameters for each of the controllers using same measurement intervals.

3.1 PID tuning

The PID controller was implemented as two independent control loops F_S-s and F_A-c_L . The velocity form of the PID controller was used for on-line control according to the following equations:

$$\begin{aligned} F_{S_n} &= F_{S_{n-1}} + K_{C1}(e_{1_n} - e_{1_{n-1}}) + \frac{K_{C1}}{\tau_{I1}} e_{1_n} \Delta t + \frac{K_{C1} \tau_{D1}}{\Delta t} (e_{1_n} + e_{1_{n-2}} - 2e_{1_{n-1}}) \\ F_{A_n} &= F_{A_{n-1}} + K_{C2}(e_{2_n} - e_{2_{n-1}}) + \frac{K_{C2}}{\tau_{I2}} e_{2_n} \Delta t + \frac{K_{C2} \tau_{D2}}{\Delta t} (e_{2_n} + e_{2_{n-2}} - 2e_{2_{n-1}}) \end{aligned} \quad (5)$$

The six control parameters were tuned by trial and error method keeping the objective of minimization of the error. The tuning parameters K_{C1} , τ_{I1} and τ_{D1} for F_S-s control loop and K_{C2} , τ_{I2} , and τ_{D2} for the F_A-c_L control loop were tuned independently. The initial values for these parameters were

determined using response curve methodology, which was then fine-tuned by minimizing output errors within the desirable range of parameters determined by simulation.

3.2 DIOLC tuning

Compared to the PID controller, the DIOLC has four tuning parameters; K_{11} and K_{12} for F_S-s control loop and K_{21} and K_{22} for F_A-c_L control loop. For the DIOLC controller the following equations were used for on-line control implementation:

$$\begin{bmatrix} v_1 \\ v_2 \end{bmatrix} = \begin{bmatrix} \dot{s} \\ \dot{c}_L \end{bmatrix} = \begin{bmatrix} \dot{s}_d + K_{11}(s_d - s) + K_{12} \int_0^t (s_d - s) dt \\ \dot{c}_{Ld} + K_{21}(c_{Ld} - c_L) + K_{22} \int_0^t (c_{Ld} - c_L) dt \end{bmatrix} \quad (6)$$

$$F_S = u_1 V, u_1 = D \quad (7)$$

$$F_A = 1553.64 \left(\frac{u_2 V^{0.2467}}{N^{1.14}} \right)^{2.5}, u_2 = k_L a \quad (8)$$

As in the case of PID tuning, the initial values for these parameters were determined using response curve methodology, which were then fine-tuned by minimizing output errors within the acceptable range, obtained from simulations. The tuning parameters for the controllers are given in Table 1.

Table 1. Tuning parameters used for PID and DIOLC

	PID			DIOLC	
$F_S - s$ Loop	$K_{C,1}$	$\tau_{I,1}$	$\tau_{D,1}$	K_{11}	K_{12}
Units	$L^2 g^{-1} h^{-1}$	h	h	h^{-1}	h^{-2}
Parameters	0.2	0.1	0.005	15	5
$F_A - c_L$ Loop	$K_{C,2}$	$\tau_{I,2}$	$\tau_{D,2}$	K_{21}	K_{22}
Parameters	15000	0.02	0.005	8	0.8

4 Materials and Methods

4.1 Culture, medium and reactor operation

The microorganism strain *S. cerevisiae* NRRL-Y-11857 was used for experiments in this study. Yeast was maintained on YM agar plates and stored at 4°C with periodic sub-culturing every month. All experiments were carried out in a 5-l bioreactor (Sartorius Biostat B Plus, Germany) maintained at pH 6, temperature 30°C and constant agitation speed of 400 rpm. Medium contained 1% yeast extract, 2% peptone and 5 g/l of initial glucose concentration. The airflow rate during the batch phase was supplied at a constant rate of 0.1 vvm. The glucose feed concentration used in fed batch mode was 125 g/l.

4.2 Analysis and data acquisition

Glucose concentration was measured in real time with the YSI-Biochemistry analyzer 2700.

Simulation experiments were carried out in MATLAB (MathWorks®). The graphical programming language LabVIEW™ (National Instruments, USA) was used to interface the reactor with the computer and develop the programme for online implementation of the PID and DIOLC controllers.

5. Results and discussion

5.1 Analysis of controller performances

We performed the validation of the PID and DIOLC controllers in two steps. First, we simulated the performance of the controllers for a square wave trajectory for glucose concentrations (Initial 1.5 hr of fed batch 4 g/l, next 1.5 hr 2 g/l and rest 1 hr 3 g/l) along with a linear trajectory for DO (from 40% to 60% during fed batch operation) executed simultaneously. This was followed by the online implementation of the same control trajectories for the fed-batch yeast fermentation process carried out in the 5-l bioreactor. The performance of the controllers under simulated and experimental conditions was examined. In Table 2, the normalized root mean square error (NRMSE) values calculated for simulations and online implementation for PID and DIOLC are presented. We observed that the NRMSE values obtained for online implementation was higher than that calculated from the simulation results for both controllers. However, DIOLC shows marginally lower values than the PID controller.

Table 2. Comparison of NRMSE values for simulation and online implementation of PID and DIOLC

s_d -square, c_{Ld} -linear	PID		DIOLC	
	s	c_L	s	c_L
Simulation (with noise & parametric perturbation)	0.41	0.16	0.39	0.11
Online Experiment	0.67	0.36	0.64	0.30

For the simulations, we implemented the following trajectory for the substrate concentration. From 4-5.35 h, substrate concentration was kept at 4 g/l, from 5.35-7 h the set point was stepped down to 2 g/l; after 7 h till the end of the experiment, the desired glucose concentration was set to 3 g/l. Simultaneously, the DO was linearly increased from 4-8 h of fermentation. These simulations were carried out in the presence of 5% random noise and 5% parametric perturbation in substrate and DO concentration to create a realistic condition.

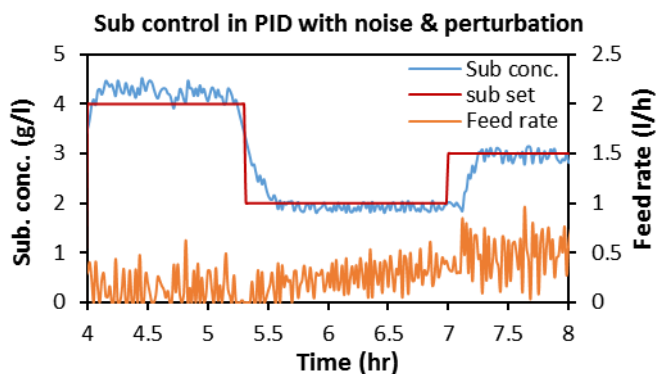


Fig. 2. Simulation showing PID performance in controlling substrate feed in presence of 5% noise and 5% of critical parameter perturbation for *S. cerevisiae* fed-batch fermentation

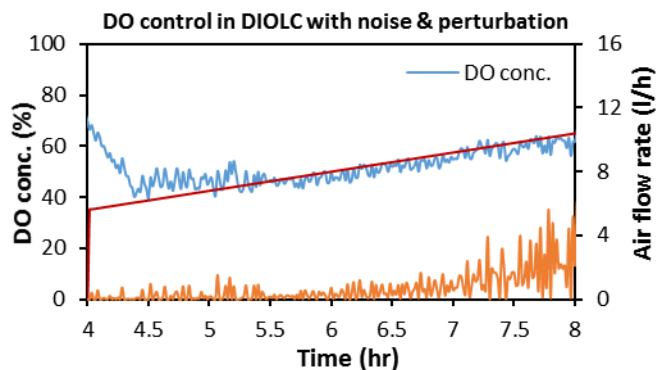


Fig. 5. Simulation showing DIOLC performance in controlling DO in presence of 5% noise and 5% of critical parameter perturbation for *S. cerevisiae* fed-batch fermentation

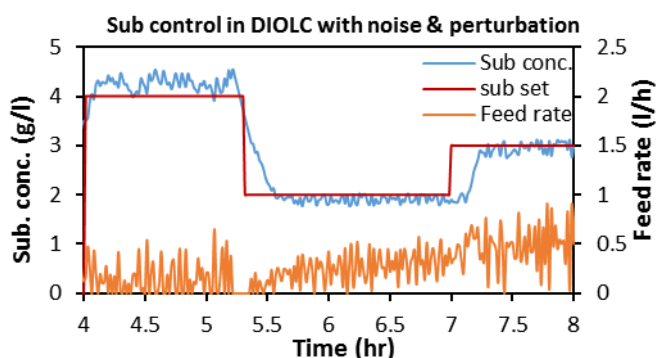


Fig. 3. Simulation showing DIOLC performance in controlling substrate feed in presence of 5% noise and 5% of critical parameter perturbation for *S. cerevisiae* fed-batch fermentation

In Figures 2 and 3, we have presented the simulation results for of the controllers for the square-wave trajectory and in Figures 4 and 5, the results for simultaneous DO control along a linear trajectory. We observed from the time profiles that the control action taken by the DIOLC was smoother than that of the PID.

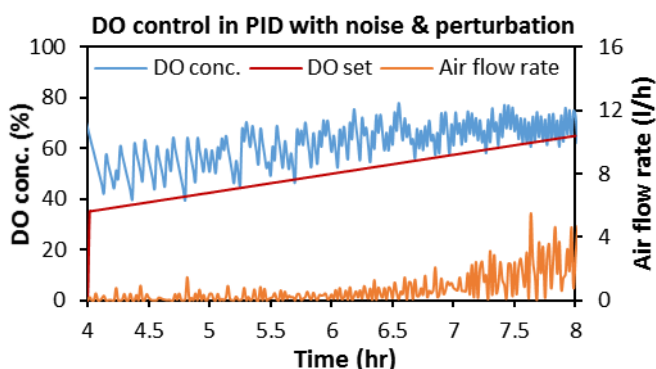


Fig. 4. Simulation showing PID performance in controlling DO in presence of 5% noise and 5% of critical parameter perturbation for *S. cerevisiae* fed-batch fermentation

5.2 Online validation of DIOLC performance

For validation of controller performance, we performed fed-batch baker's yeast fermentation experiments as delineated in the Materials and Methods. In Figures 6 to 9, we present the results of the online control implementation of PID and DIOLC controllers. The same square-wave trajectory for substrate and linear trajectory for oxygen was imposed on the process.

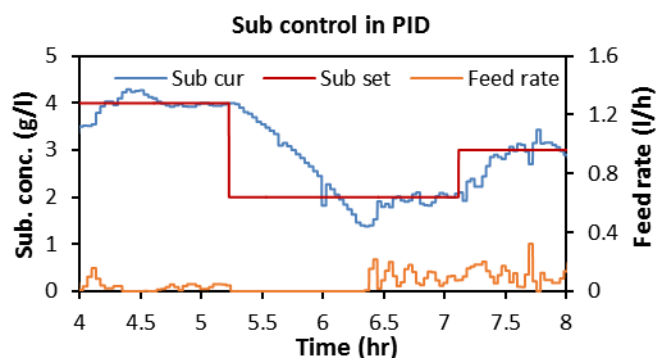


Fig. 6. PID performance in controlling substrate feed in *S. cerevisiae* fed-batch fermentation

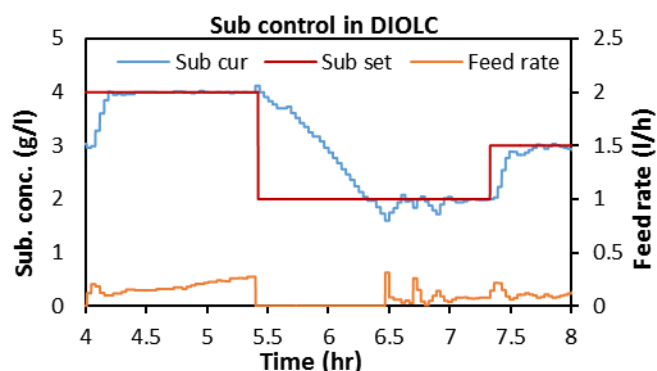


Fig. 7. DIOLC performance in controlling substrate feed in *S. cerevisiae* fed-batch fermentation

From Figures 6 and 7, we can compare substrate control action for PID and DIOLC. We observe that control action during the step down segment of the trajectory for substrate control, the substrate concentration decreases gradually. The reason for this is that the glucose is consumed based on the metabolic state of the cells, the residual concentration of glucose in the medium and the dissolved oxygen concentration. Although, the trend of decrease is similar in both Figures 6 and 7, these are significantly different from the corresponding simulation results (Figures 2 and 3). The control action observed for the DIOLC is better. Both controllers correctly discontinue addition of feed during the step down phase of the substrate trajectory.

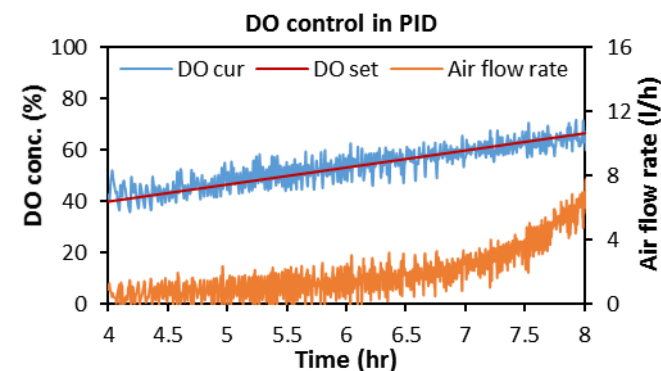


Fig. 8. PID performance in controlling DO in *S. cerevisiae* fed-batch fermentation.

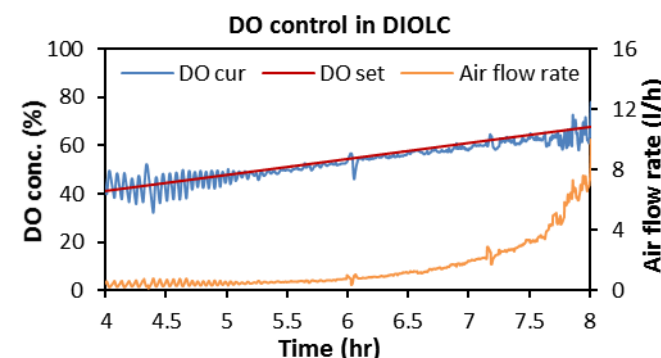


Fig. 9. DIOLC performance in controlling DO in *S. cerevisiae* fed-batch fermentation.

Figures 8 and 9 show the controller performance in simultaneously maintaining the DO along a linear trajectory. It was observed that the PID control action is more sensitive to the process noise compared to the DIOLC controller. Further, the DO concentration is far more oscillatory. In the case of the DIOLC, it is clear that the algorithm converges to the solution curve.

6. Conclusions

A model for growth of *S. cerevisiae* was used to develop the DIOLC for the process and its performance was benchmarked with a PID controller. It was observed in simulations that the overall performance of DIOLC was better than the PID for test trajectories that included rapid square wave changes of one of the variables while the other was changing linearly and

when the significant parameters to which the process was sensitive, were perturbed. The online implementation of these trajectories in a fed batch reactor showed that the DIOLC performed better in terms of both control action taken as well as the resulting output time profiles.

7. Acknowledgements

The authors gratefully acknowledge the Department of Science and Technology, GOI, for funding this project. VC gratefully acknowledges CSIR for SRF fellowship.

8. Appendix

Table 3. Description of parameters and their values used in DOE analysis and in the model used for simulations [Persad, A. et al. 2013].

Parameter	Description	Values
$q_{S,max}$ (g/l)	Maximal specific glucose uptake rate	3.50
$q_{O_2,max}$ (mg/l)	Maximal specific oxygen uptake rate	8.00
$Y_{biomass/glucose}^{oxidative}$ (g/g)	Oxidative yield of biomass on glucose	0.49
$Y_{biomass/glucose}^{reductive}$ (g/g)	Reductive yield of biomass on glucose	0.05
OX (mole/mole)	Oxygen content of biomass in molecular formula	0.57
$Y_{biomass/ethanol}$ (g/g)	Oxidative yield of biomass on ethanol	0.70
$\mu_{max,ethanol}$ (1/h)	Maximal specific growth rate	0.17
K_s (g/l)	Saturation parameter for glucose uptake	0.30
K_o (mg/l)	Saturation parameter for oxygen uptake	0.10
K_e (g/l)	Saturation parameter for growth on ethanol	0.10
K_i (g/l)	Inhibition parameter for ethanol uptake	0.10
HX (mole/mole)	Hydrogen content of biomass in molecular formula	1.79
NX (mole/mole)	Nitrogen content of biomass in molecular formula	0.15
a (mole/gram)	Moles of oxygen used per gram of glucose	0.014
k (mole/gram)	Moles of oxygen used per gram of ethanol	0.037
k_{La} (1/hr)	Mass transfer coefficient	50

9. References

- Karakuzua, C., Türker, M., Öztürk, S. (2006). Modelling, on-line state estimation and fuzzy control of production scale fed-batch baker's yeast fermentation *Control Engineering Practice*. 14: 959–974.
- Kasperski, A., & Miśkiewicz, T. (2008). Optimization of pulsed feeding in a Baker's yeast process with dissolved

oxygen concentration as a control parameter. *Biochemical Engineering Journal*. 40(2): 321-327.

Ławryńczuk, M. (2011). Online set-point optimisation cooperating with predictive control of a yeast fermentation process: A neural network approach. *Engineering Applications of Artificial Intelligence*. 24: 968–982.

Miśkiewicz, T. and Borowiak, D. (2005). A logistic feeding profile for a fed-batch Baker's yeast process. *Electronic Journal of Polish Agricultural University*. 8: 1-13.

Ostergaard, S., Olsson, L., and Nielsen, J. (2000). Metabolic engineering of *Saccharomyces cerevisiae*. *Microbiology and Molecular Biology Reviews*. 64(1): 34-50.

linearizing controller and linear interpolation PID controller: Enhancing Biomass and Ethanol production in *Saccharomyces cerevisiae*. *Applied biochemistry and biotechnology*. 169(4): 1219-1240.

Renard, F., Wouwer, A. V. (2008) Robust adaptive control of yeast fed-batch cultures *Computers and Chemical Engineering*. 32:1238–1248.

Sonnleitner, B. and Kappeli, O. (1986). Growth of *Saccharomyces cerevisiae* is controlled by its limited respiratory capacity: Formulation and Verification of a hypothesis. *Biotechnology and Bioengineering*. 28, 927-937.

Persad, A., Chopda, V. R., Rathore, A. S., and Gomes, J. (2013). Comparative performance of decoupled input–output